Journal of the Korea Institute of Applied Superconductivity and Cryogenics
Vol.5,No.1, (2003),pp. 21~26

A semispherical SQUID magnetometer system using high sensitivity double relaxation oscillation SQUIDs for magnetoencephalographic measurements

Yong-Ho Lee, Hyukchan Kwon, Jin-Mok Kim, Kiwoong Kim, and Yong-Ki Park

Korea Research Institute of Standards and Science

Yhlee@kriss.re.kr

Abstract--**We designed and constructed a multichannel superconducting quantum interference device (SQUID) magnetometer system to measure magnetic fields from the human brain. We used a new type of SQUID, the double relaxation oscillation SQUID (DROS). With high flux-to-voltage transfers of the DROS, about 10 times larger than the dc SQUIDs, simple flux-locked loop circuits could be used for SQUID operation. Also the large modulation voltage of the DROS, typically being 100 μV, enabled stable flux-locked loop operation against the thermal offset voltage drift of the preamplifier. The magnetometers were fabricated using the Nb/AlO_x/Nb junction technology. The SQUID system consists of 37 signal magnetometers, distributed on a semispherical surface, and 11 reference channels were installed to pickup background noises. External feedback was used to eliminate the magnetic coupling with the adjacent channels. The liquid helium dewar has a capacity of 29 L and boil-off rate of about 4 L/d with the total 48 channel insert. The magnetometer system has an average noise level of 3 fT/√Hz at 100 Hz, inside a shielded room, and was applied to measure auditory-evoked fields.**

1. INTRODUCTION

Measurements of the magnetic fields from the human brain provide useful information for the diagnoses of brain functions. Many superconducting quantum interference device (SQUID) systems were developed for measuring the magnetoencephalogram (MEG) signals [1, 2]. Since the magnetic field strengths of these MEG signals are usually weak than 1 pT, low-noise SQUIDs are necessary. SQUIDs made of low temperature superconductors, typically Nb, are the most sensitive low-frequency magnetic field sensors available, and have enough field sensitivity for measuring most of the MEG signals. However, the conventional DC SQUIDs have small flux-to-voltage transfer coefficients, typically about 100 $\mu V/\Phi_0$ (Φ_0 the flux quantum, 2.07×10^{-15} Wb). Thus the SQUID sensitivity is limited by the input noise of the room-temperature preamplifier if the SQUID output voltage is measured directly with the preamplifier. In order to detect the SQUID output voltage without a degradation of the SQUID sensitivity by the preamplifier, a very low-noise preamplifier or ac flux modulation, matching circuit and phase sensitive detection are usually used [3].

In order to operate SQUID sensors with simple electronics, the SQUID should have large flux-to-voltage transfer coefficients such that a room-temperature preamplifier can measure the SQUID output voltage directly. Several types of SQUID were introduced to increase the transfer coefficients. Among them, double relaxation oscillation SQUIDs (DROSs) provides more than 10 times larger transfer coefficients, compared with the standard dc SQUID, and large modulation voltages. Therefore, simple flux-locked loop electronics could be used for SQUID operation [4].

To measure MEG signals from a certain part of the brain more accurately, we need a multichannel with having as many sensors as possible and the dewar tail or sensor distribution need to be optimized for the head shape. The Helmet-type system can measure the field distribution of the whole head at the same time, but the fabrication and maintenance need lots of work. A semispherical system with optimized sensor distribution to fit the local curvature of the head can measure the field distribution with shorter sensor-to-source distances, resulting in higher signal-to-noise ratios, and the fabrication of a middle scale system is much easier than the whole-head systems [5].

The motivation of the present study is to fabricate a compact MEG system with simple electronics. The SQUID system has a semispherical sensor distribution, and SQUID sensors are based on DROS magnetometers. The fabrication and operation results of the system are described.

2. DROS MAGNETOMETER

2.1. Operation condition of DROS

In contrast to the DC SQUID, the DROS uses unshunted hysteretic tunnel junctions. The schematic circuit drawing of the DROS is shown in Fig. 1(a). The DROS consists of a hysteretic dc SQUID (the signal SQUID) and a hysteretic junction (the reference junction), shunted by a relaxation

circuit of a resistor R_{sh} and an inductor L_{sh}. Instead of the original reference SQUID, we used the reference junction to remove the possibility of flux trapping by the reference SQUID and to reduce wires for SQUID operation [6].

In a dc bias current I_b, high frequency relaxation oscillations can occur with an oscillation frequency of about R_{sh}/L_{sh}. During the oscillations, either the signal SQUID or reference junction participates in the oscillation, and the other stays at the zero voltage state. If we use a preamplifier with a bandwidth much narrower than the oscillation frequency, time-averaged dc voltage appears. The critical current of the signal SQUID changes by applying flux through it, but the reference critical current is fixed. Fig. 1(b) shows the modulation of the signal critica

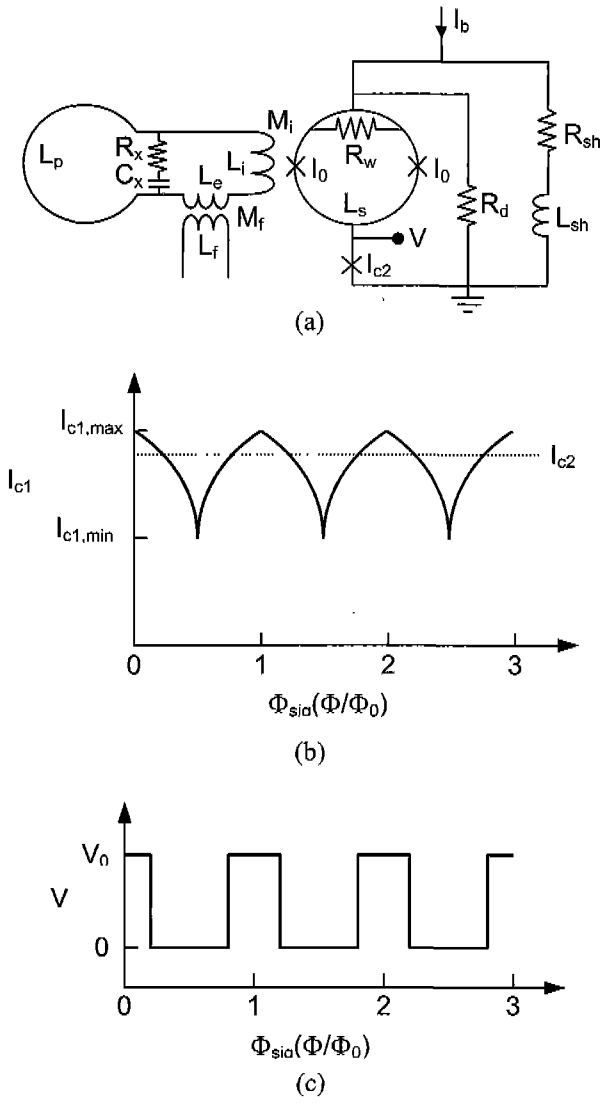

Fig. 1. Structure and operation principle of the DROS. (a) Schematic circuit drawing of the DROS, (b) modulation of the signal critical current versus the signal flux, and (c) flux-voltage curve for a fixed reference critical current I_{c2}. $I_{c1,max}$ is equal to $2I_0$.

current with signal flux. The reference critical current I_{c2} should be in-between $I_{c1,max}$ and $I_{c1,min}$. If $I_{c1} > I_{c2}$, the reference junction participates in the relaxation oscillations, and since we measure the output voltage across the reference junction, voltage drop appears across the reference junction. On the other hand, if $I_{c1} < I_{c2}$, the signal SQUID participates in the oscillation, and the reference junction stays in the superconducting state, resultin in no voltage output. If the flux value is changed that $I_{c1} = I_{c2}$, the two critical currents have equal probability to oscillation, and abrupt voltage output appears with large flux-to-voltage transfer coefficient as shown in Fig. 1(c).

2.2. Structure of DROS magnetometer

The overall structure of the magnetometer is shown in Fig. 2(a). The size of the magnetometer is 16 mm × 10 mm, and the pickup coil has a linewidth of 0.5 mm. In order to eliminate magnetic cross-talk with the adjacent channels, external feedback scheme was used. The feedback coil is formed on the opposite side of the magnetometer as shown in Fig. 2(a). The mutual inductance between the feedback coil and flux transformer M_f is 3 nH. In the lower part of the magnetometer, there are DROS and damping circuits.

The closeup view of the DROS is shown in Fig. 2(b). The signal SQUID is a Ketchen-type DC SQUID with two square holes connected in parallel. By using parallel connection, we could reduce input coil turns necessary for the inductance matching with the pickup coil. Each square hole has an inner dimension of 100 μm × 100 μm. The total SQUID inductance was estimated to be 104 pH, including the parasitic inductance due to the slit structure and junction inductance. The Josephson junctions in the signal SQUID have sizes of 4 μm × 4 μm each, whereas the reference junction has a size of 5 μm × 5 μm. In terms of the area ratio, the reference critical current corresponds to 78 % of the maximum value of the signal critical current, which is near the mid point of the modulation range of the signal critical current when modulation parameter β_L is 1. The input coil consists of two series-connected coils, 10-turns each with a linewidth of 5 μm, integrated on each SQUID loop and the input coil inductance is calculated to be 37 nH. The mutual inductance between the input coil and the SQUID is estimated to be 1.76 nH. The pickup coil has linewidth of 0.5 mm and size of 16 mm × 10 mm. The inductance of the pickup coil is calculated to be 40 nH and the field-to-flux transfer of the flux transformer circuit was calculated to be 0.56 nT/Φ_0.

Since the intrinsic noise of the DROS is inversely proportional to the square root of the relaxation frequency, the relaxation frequency was designed to be as high as about 1 GHz. With the reference critical current of 10 μA, the intrinsic flux noise of the DROS is calculated to be 1 $\mu\Phi_0/\sqrt{\text{Hz}}$. The shunt inductor consists of two figure-of-eight coils, connected in series and formed symmetrically with respect to the signal SQUID to eliminate magnetic coupling with the signal SQUID.

In order to provide the stable operation condition of the DROS, some damping circuits were used. First, since the DROS has hysteretic junctions, a parasitic resonance due to the junction capacitance and the shunt inductance L_{sh} can

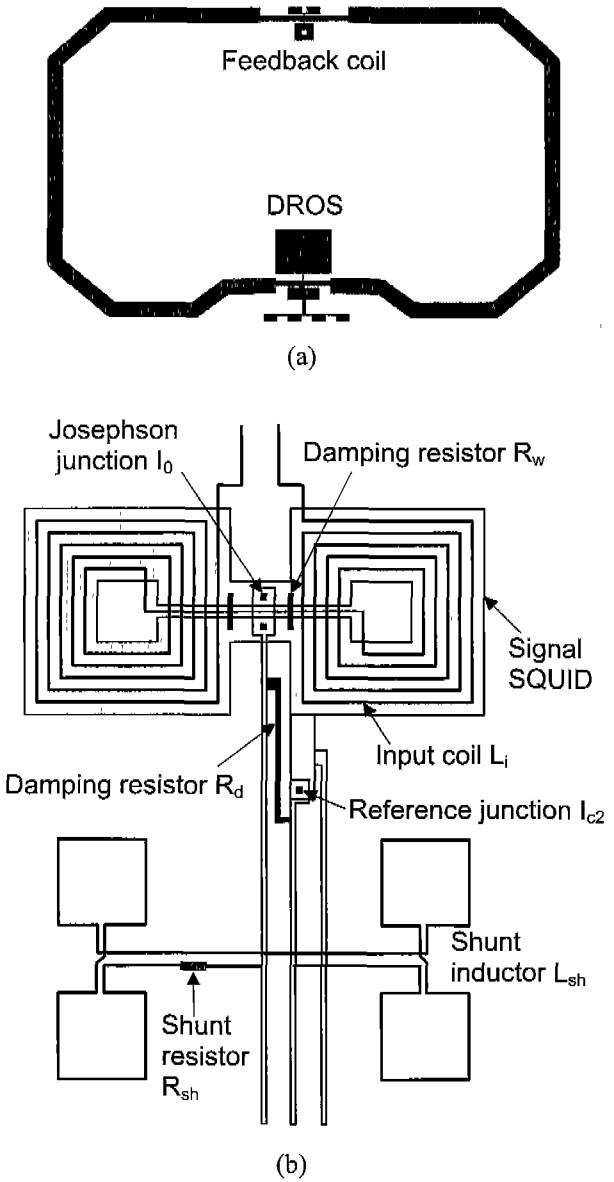

Fig. 2. Design of the DROS magnetometer. (a) Structure of the magnetometer, and (b) details of the DROS.

occur. To damp this LC resonance, a damping resistor R_d was used across the signal SQUID and the reference junction [7]. Second, the signal SQUID washer acts a ground plane for the input coil, giving rise to a resonance. To damp this washer resonance, a damping resistor R_w was inserted across the signal SQUID loop [8]. Third, a damping circuit made of a resistor R_x and a capacitor C_x was put in the flux transformer to damp the resonance in the input coil, and to filter out high-frequency noise from the pickup coil. Damping circuit made of a resistor(20 Ω) and a capacitor(0.4 nF) was put in the flux transformer to damp resonance in the input coil. The resonance factor of the flux transformer is 0.35, which is low enough for the

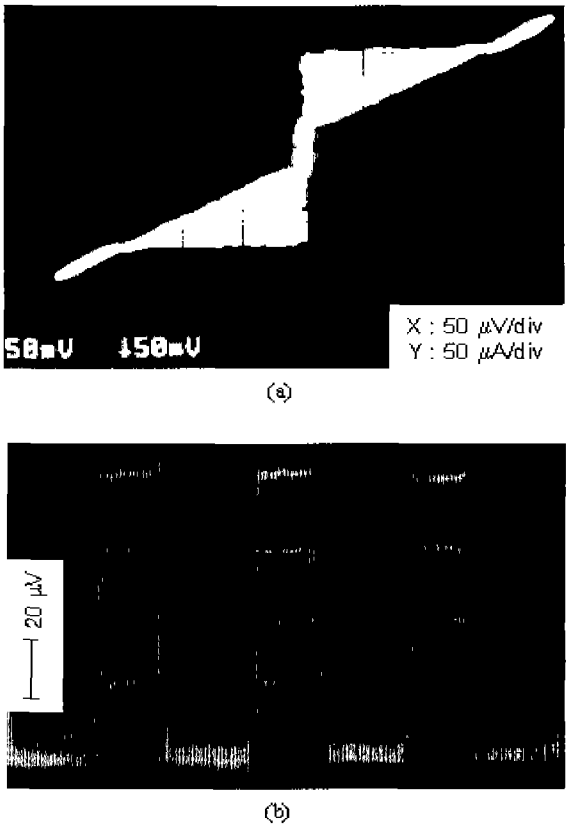

efficient damping.

Fig. 3. (a) Modulated current-voltage curves of the DROS where a flux of about $2\Phi_0$ is applied during sweeping, and (b) flux-voltage curves at 4 bias currents.

2.3. Fabrication of magnetometers

Since the DROS magnetometers are based on hysteretic low-T_c junctions, sensors were fabricated using the Nb/AlO_x/Nb junction technology. The Nb/AlO_x/Nb trilayers were deposited by dc magnetron sputtering, and the junction areas were defined by reactive ion etching. The insulator between metal layers is an SiO_2 film deposited by plasma-enhanced chemical vapor deposition. The resistor is made of reliable Pd thin film. The overall size of the magnetometer is 17 mm × 12 mm, and 14 magnetometers were fabricated together on 3-inch Si wafer. We used the 4-level process with 5 photomasks. The fabricated magnetometers were glued onto printed circuit board sensor holders having a diameter of 22 mm, where wiring copper leads were printed with nonmagnetic connectors. Each magnetometer holder has a plastic protective cap for hermetic sealing and easy-handling, allowing quick attachment or removal from the multichannel insert. Wirings between the magnetometers and holders were made using ultrasonic Al-wire bonding.

2.4. Characterization of magnetometers

The magnetometers were cooled by inserting directly into a fiberglass liquid helium dewar. Measurements were done inside a magnetically shielded room (MSR) with two layers of Mu-metal and one layer of Al, which has shielding factors of about 60 dB at 1 Hz and 90 dB at 100 Hz . Fig. 3(a) shows flux modulated current-voltage curve, where a flux of about 2 Φ_0 at a frequency of 5 times the current
sweeping frequency was applied. The magnetometers had reference critical currents of 10-20 μA, and the maximum modulation voltages of around 120 μV, which is more than 2 times larger than DC SQUIDs. The flux-voltage curves showed almost a step function of the applied field as shown in Fig. 3(b). The maximum flux-to-voltage transfers were around 1 mV/Φ_0, which is about 10 times larger than the transfer of standard DC SQUIDs. Using a calibration field coil, the field-to-flux transfer coefficient of the flux transformer was measured to be 0.54 nT/Φ_0, quite close to the design value of 0.56 nT/Φ_0.

3. SEMISPHERICAL MAGNETOMETER SYSTEM

3.1. Readout electronics

The single channel electronics for flux-locked loop (FLL) operation and SQUID control consist of a dc bias current, preamplifier, main amplifier, integrator and control circuits. Since the fabricated DROS magnetometers had large flux-to-voltage transfers, the DROS output voltage could be measured directly by room-temperature dc preamplifiers without using matching circuits and ac flux modulation.

Using the common LT1028 (Linear Technology) operational amplifiers, DC preamplifiers were constructed. The input voltage noise of the preamplifiers was about 1.5 nV/√Hz at 100 Hz. With a typical transfer coefficient of 1 mV/Φ_0, the preamplifier contributes an equivalent flux noise of 1.5 μΦ_0/√Hz at 100 Hz. Since the flux noise is typically 5 μΦ_0/√Hz at 100 Hz, the relative contribution of the preamplifier to the total SQUID system noise is about 10 %. Due to the large modulation voltage of DROSs, the FLL operation was quite stable against the offset voltage drift of the amplifier chain. The operation margin for the offset drift is about ±15 μV around the center of modulation voltage.

The control of the SQUID operation could be done either manually or automatically. In the automatic mode, the software controls the bias current, the voltage offset at the integrator, and the flux bias. The optimum bias current was determined by the measured white noise. The electronics of the magnetometer system consists of 6 boxes for FLL circuits and 3 sub-racks for SQUID controls. Each head box has 8 modular FLL circuits and was fixed on the ceiling of the MSR. The control electronics are within a RF-shielded Al cabinet located outside the MSR. The FLL outputs can be passed selectively through 0.3-Hz high pass filters, 100-Hz low pass filters and 60-Hz notch filters, and gain-adjustable amplifiers.

Fig. 4(a) shows the typical field noise spectrum of the magnetometers when the magnetometer was operated inside the MSR without using an additional superconductive shield. Including all the noise contributions, like the residual magnetic noise of the MSR and the dewar thermal noise, the SQUID system noise is about 3 fT/√Hz at 100 Hz. Hanning window was used and data were averaged 10 times. Several noise peaks around 10 Hz and 20 Hz are due to mechanical vibrations of the magnetometer in the residual magnetic field of the MSR which is about 20 nT. Fig. 4(b) shows the field noise versus the modulation voltage. At low modulation voltage, the preamplifier input noise contributes to the total noise. The noise is minimal at the modulation voltage of around 80 μV and increases with modulation voltage. It seems that noise decreases above 110 μV, but the FLL operation becomes very unstable near 120 μV.

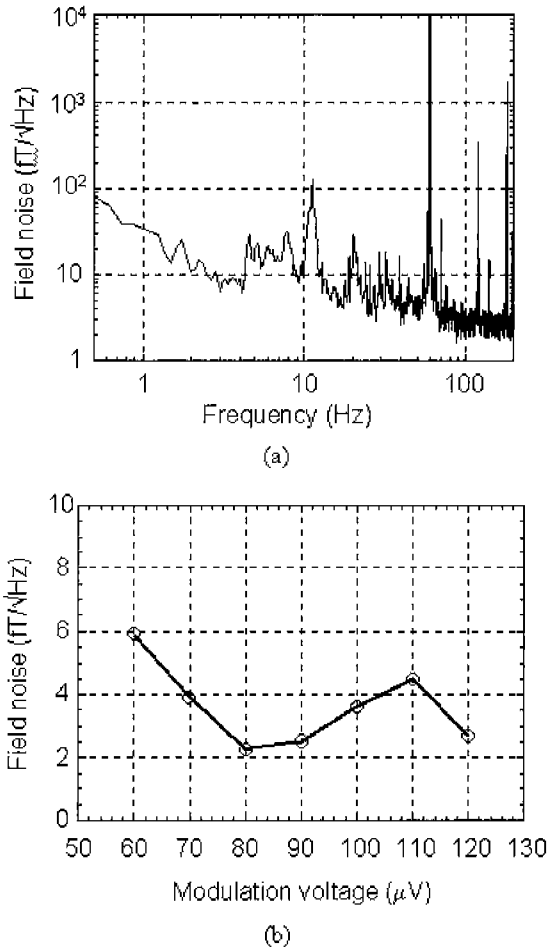

Fig. 4. (a) Magnetic field noise spectrum of the DROS magnetometer measured inside a magnetically shielded room, and (b) field noise versus the modulation voltage. The peaks around 10 Hz and 20 Hz are caused by mechanical vibrations of the magnetometer in the residual magnetic field.

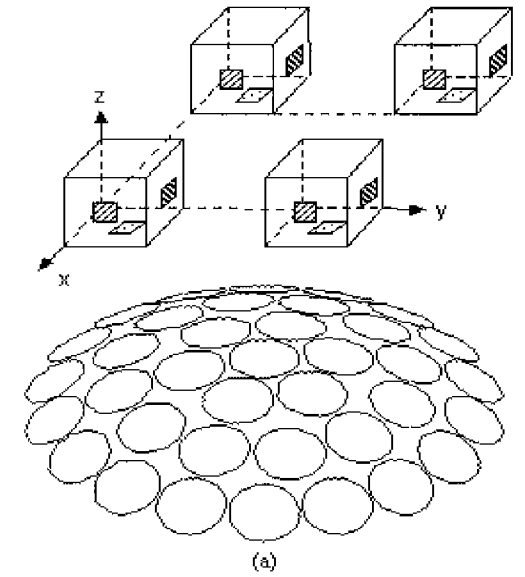

(a)

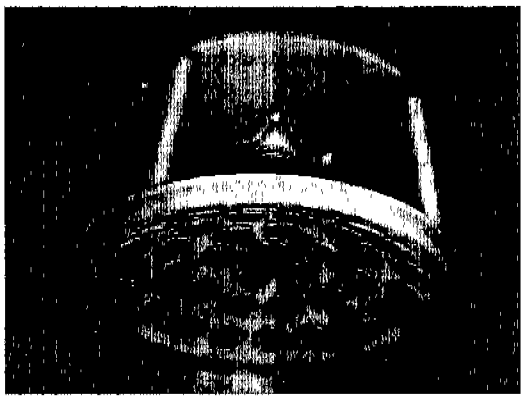

(b)

Fig. 5. (a) Schematic drawing of the 37 signal channels and 11 reference channels, and (b) photograph of the insert

3.2. Semipherical 37 channel insert

The magnetometer system consists of 37 magnetometers to measure MEG signals and noise fields at the same time, and 11 reference magnetometers to measure noise fields only. Fig. 5(a) shows the schematic drawing of the 37 signal channels and 11 reference channels. The 37 magnetometers were distributed on a semispherical surface with a radius of 125 mm and measure the field component normal to the head surface. The distance between adjacent magnetometers is 26 mm, and the 37 channels cover 160 mm in diameter. The 11 reference magnetometers are arranged to measure 3 components of the magnetic fields, and are located between 50 mm and 90 mm above the signal channels. Since the reference channels pickup background noises only, we can apply adaptive filtering or software gradiometer to eliminate background noises. Using the 11 reference channels, it is possible to measure 3 vector fields, B_x, B_y, and B_z, and 5 first-order gradients, dB_x/dx, dB_x/dy, dB_x/dz, dB_y/dy, and dB_y/dz. By combining these field components and first-order gradient components, second-order software gradiometers can be formed. Fig. 5 (b) shows the photograph of the fabricated SQUID insert. In order to reduce the thermal load, nonmagnetic fiberglass tubes were used to support the SQUID supports, and radiation baffles made of Cu plate and styrofoam were used for the thermal shield at the dewar neck.

4. Operation of 37-channel system

4.1. Neuromagnetic measurement system

The SQUID system consists of 37 signal channels, 11 reference channels, cryogenic insert, liquid helium dewar, dewar gantry, FLL circuits, SQUID controllers, MSR, RF-shielded cabinet, signal processing, and source localization software. The liquid helium dewar has a liquid volume of 29 L and the boil-off rate of the liquid helium is about 3.5 L/d with the insert. To minimize thermal magnetic noise, the multilayer superinsulation was made of island structure Al films with an island size of 8 mm × 8 mm. The thermal shield is made of Cu wires to minimize thermal noise. The contribution of dewar thermal noise to the system noise was measured to be lower than 2 fT/$\sqrt{\text{Hz}}$ at 100 Hz. The distance between the room temperature and the liquid helium is 20 mm. The dewar gantry was made of fiberglass, aluminum, and brass. The dewar can be moved in the vertical direction, and also can be tilted.

4.2. Application to neuromagnetic measurements

To demonstrate the usefulness of the developed system for measuring MEG signals, the 37-channel magnetometer system was applied to measure auditory-evoked fields. The software for the neuromagnetic measurements consists of DC offset removal, low-pass filter, 60-Hz elimination filter, averaging, synthetic software gradiometer, field mapping and source localization. To apply non-magnetic auditory stimuli, a capacitive earphone was used with the auditory signal lines twisted in pair. Auditory stimuli of a 1-kHz tone burst, 170-ms duration, and about 70-dB normal hearing level were applied to the right ear of a normal human subject in a random interval, and fields were measured over the left temporal lobe. Sampling rate was 500 Hz. Fig. 6 shows the auditory-evoked responses with the traces superposed together. The traces were obtained by applying the modified principal component elimination method [9], averaging of 100 times, and a digital 40-Hz low pass filter. The high-pass, low-pass and 60-Hz elimination filters in the SQUID controllers were not used in this measurement.

The N100m peak, the field component generated at about 100 ms after the stimulus onset, was obtained. This peak corresponds to the primary response of the auditory cortex to the sound stimulus. The signal was obtained without using the software gradiometer, and the average signal to noise ratio of the N100m peaks is about 7. Fig. 7 shows the isofield contour map of the N100m peak. The field distribution at this peak shows dipolar field pattern due to the primary auditory cortex.

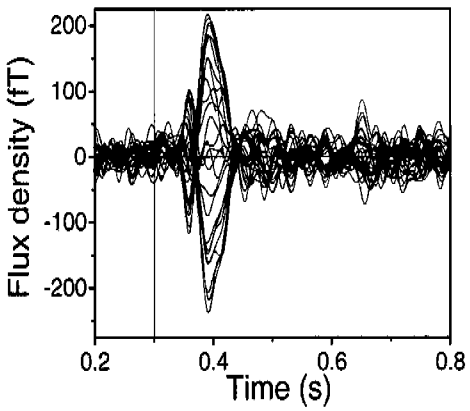

Fig. 6. Multichannel traces of auditory-evoked field signals. The stimulus starts at 0.3 s and ends at 0.47 s.

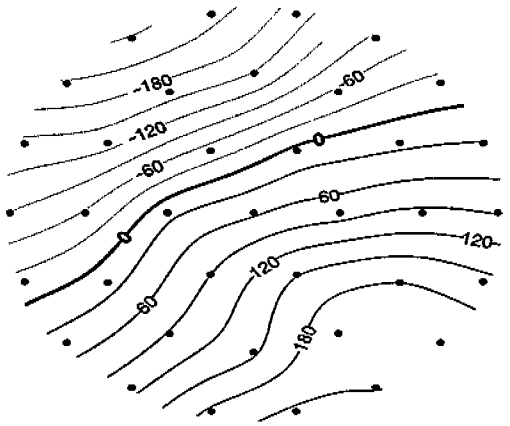

Fig. 7. Isofield contour map of the auditory-evoked response at a latency of N100m. The thin, thick, and gray lines indicate the magnetic flux flowing out of the head, zero flux, and flowing into the scalp, respectively. The field unit is fT.

5. Conclusion

We constructed a semispherical magnetometer system based on DROS magnetometers, and applied to measure neuromagnetic fields. Due to the flux-to-voltage transfers of the DROSs, about 10 times larger than those of dc SQUIDs, compact electronics could be used for SQUID operation. The contribution of the preamplifier input noise was about 10 % of the system noise. The large modulation voltage of DROSs allowed stable FLL operation against the thermal drift of the amplifier voltage offset. By reducing the thermal noise of the dewar, the dewar noise is less than 2 fT/$\sqrt{\text{Hz}}$ at 100 Hz. The average noise level of the magnetometer system is about 3 fT/$\sqrt{\text{Hz}}$ at 100 Hz, which is low enough for neuromagnetic measurements. By software gradiometers using the reference magnetometers, we can expect some reduction of vibrational noise peaks. By using the 37-channel system, neuromagnetic fields evoked by auditory stimuli were successfully measured. Using the developed semispherical magnetometer system, we measured auditory-evoked fields and could get an isofield field mapping, implying that DROS magnetometers can be used in multichannel systems with compact SQUID electronics.

Acknowledgment

This work was supported by the NRL project of the Ministry of Science and Technology, Korea.

References

[1] M. Hämäläinen, R. Hari, R. J. Ilmoniemi, J. Knuutila, O. V. Lounasmaa. Magnetoencephalography- theory, instrumentation, and applications to noninvasive studies of the working human brain *Rev. Mod. Phys.* 1993;65:413-497.

[2] J. P. Wikswo, Jr. SQUID magnetometers for biomagnetism and nondestructive testing: Important questions and initial answers. *IEEE Trans. Appl. Supercond.* 1995;5:74-120.

[3] D. Drung. Advanced SQUID readout electronics. in *SQUID Sensors: Fundamentals, Fabrication and Application.* ed. H. Weinstock, Dordrecht, Kluwer Academic Publishers, 1996. p. 63-116.

[4] D. J. Adelerhof, H. Nijstad, F. Flokstra, and H. Rogalla. (Double) relaxation oscillation SQUIDs with high flux-to-voltage transfer: Simulations and experiments. *J. Appl. Phys.* 1994;76:3875-3886.

[5] Y. Hirata and S. Kuriki. Modular middle-scale SQUID magnetometer system for neuromagnetic research. *IEEE Trans. Electron.* 1996;E79-C:1213-1218.

[6] [6] Y. H. Lee, H. C. Kwon, J. M. Kim, Y. K. Park, and J. C. Park. Double relaxation oscillation SQUID with reference junction for biomagnetic multichannel applications. *Appl. Supercond.* 1998;5:413-418.

[7] D. J. Adelerhof, J. Kawai, G. Uehara, and H. Kado. High sensitivity double relaxation oscillation superconducting quantum interference devices with large transfer from flux to voltage. *Rev. Sci. Instrum.* 1995;66:2631-2637.

[8] [8] R. Cantor. DC SQUIDs: Design, optimization and practical applications. in *SQUID Sensors: Fundamentals, Fabrication and Application.* ed. H. Weinstock, Dordrecht, Kluwer Academic Publishers, 1996. p. 179-233.

[9] K. Kim, Y. H. Lee, H. Kwon, J. M. Kim, C. S. Kang, Y. K. Park and I. S. Kim. Correction in the principal component elimination method for excluding correlated noises in neuromagnetic evoked field measurements. Submitted to *IEEE Trans. Biomed. Eng.* 2002.